

Proceeding Paper

# Synthesis and Characterization of a Bifunctional Platform Based on Magnetite–Gold Nanoparticles for Theranostics of Cancer <sup>†</sup>

Iuliia Chudosai <sup>1,2,\*</sup>, Marina Sorokina <sup>2,\*</sup>, Maxim Abakumov <sup>2,3</sup>  and Natalia Klyachko <sup>1</sup> 

<sup>1</sup> Faculty of Chemistry, M.V. Lomonosov Moscow State University, 119991 Moscow, Russia; nklyachko@gmail.com

<sup>2</sup> College of New Materials and Nanotechnologies, National University of Science and Technology (MISIS), 117049 Moscow, Russia; abakumov1988@gmail.com

<sup>3</sup> Department of Medical Nanobiotechnology, Pirogov Russian National Research Medical University, 117997 Moscow, Russia

\* Correspondence: chudosay@gmail.com (I.C.); sorokina.marina.a98@gmail.com (M.S.)

<sup>†</sup> Presented at the 4th International Online Conference on Nanomaterials, 5–19 May 2023; Available online: <https://iocn2023.sciforum.net>.

**Abstract:** One of the most interesting objects in terms of use in biomedicine are hybrid structures based on magnetic nanoparticles (NPs) and NPs of noble metals, which make it possible to simultaneously introduce two types of ligands onto the surface of NPs for their further use for photodynamic cancer therapy (PDT) (a combination of a photosensitizer (PS) for therapy and a fluorophore (FP) for platform detection). The synthesis and research of Fe<sub>3</sub>O<sub>4</sub>-Au NPs with a “dumbbell” structure as the bifunctional platform for the therapy of oncological diseases was the purpose of this work.

**Keywords:** nanomaterials; targeted therapy; magnetite; PDT; photosensitizer; fluorophore; FRET; theranostics



**Citation:** Chudosai, I.; Sorokina, M.; Abakumov, M.; Klyachko, N. Synthesis and Characterization of a Bifunctional Platform Based on Magnetite–Gold Nanoparticles for Theranostics of Cancer. *Mater. Proc.* **2023**, *14*, 72. <https://doi.org/10.3390/IOC2023-14498>

Academic Editor: Antonio Di Bartolomeo

Published: 5 May 2023



**Copyright:** © 2023 by the authors. Licensee MDPI, Basel, Switzerland. This article is an open access article distributed under the terms and conditions of the Creative Commons Attribution (CC BY) license (<https://creativecommons.org/licenses/by/4.0/>).

## 1. Introduction

Recently, the synthesis and characterization of dimeric nanoparticles (NPs) as a bifunctional platform have attracted much research attention [1–4]. This structure provides two functional surfaces for the attachment of different types of molecules, which makes these nanoparticles particularly attractive as multifunctional probes for diagnostic and therapeutic purposes [5,6]. Dumbbell-type Fe<sub>3</sub>O<sub>4</sub>-Au NPs are one such multifunctional system. They contain both gold and magnetite nanoparticles, which are biocompatible and widely used in biomedicine for optical and magnetic applications [7–10]. Compared to conventional single-component Au or Fe<sub>3</sub>O<sub>4</sub> nanoparticles, dimeric Fe<sub>3</sub>O<sub>4</sub>-Au NP systems have several advantages: (1) this structure contains both magnetic (Fe<sub>3</sub>O<sub>4</sub>) and optically active (Au) parts and is suitable for simultaneous optical and magnetic monitoring; (2) the presence of two surfaces in Fe<sub>3</sub>O<sub>4</sub>-Au NPs enables the attachment of different chemical functional groups; (3) both magnetite and gold dimensions can be controlled to optimize magnetic and optical properties.

All the above advantages of Fe<sub>3</sub>O<sub>4</sub>-Au NPs enable their use as a bifunctional platform. In a number of publications [1,7,9], they are proposed to be used for the treatment of cancer from hyperthermia, transportation and targeted drug delivery, the enhancement of image contrast in MR imaging, photodynamic therapy (PDT), etc.

The advantage of nanoparticles is determined by their size, restored with the size of intracellular biological objects. A high ratio of surface area to volume of nanoparticles is immediately detected makes it possible to create complex nanoplatforms and is registered in therapeutic and diagnostic areas. One such platform is the magnetite–gold bifunctional platform. Because of their magnetic properties, magnetic nanoparticles can be targeted

and held at the site of action of an external magnetic field, which is used for magnetic hyperthermia and targeted drug delivery. Magnetite nanoparticles have significant superparamagnetic properties in significant quantities and can be used as a contrast agent indicator in magnetic resonance imaging (MRI). Gold nanoparticles are special.

Relevant for diagnostics is the detection of pronounced plasmon resonance. Due to the formation of a strong sulphur-gold covalent bond, the processing of gold nanoparticles facilitates the functionalisation of sulphur-containing thiol ligands and disulphides. Combining magnetite and gold nanoparticles into one system certainly uses each of the types of nanoparticles. The bifunctional magnetite–gold system with external modifications of two types of ligands can be used simultaneously for the photodynamic therapy of cancer (PDT) and fluorescent diagnostics.

Therefore, the aim of this work is to synthesize and characterize dumbbell-shaped modified dimeric  $\text{Fe}_3\text{O}_4$ -Au NPs containing photosensitizers (PSs) on the magnetite surface and fluorophores (FPs) on the gold surface to enable the combined use of photodynamic therapy (PDT) and fluorescent diagnosis (FD) for cancer therapy.

## 2. Materials and Methods

A scheme of stepwise modification of the  $\text{Fe}_3\text{O}_4$ -Au NP bifunctional platform is shown in Figure 1.

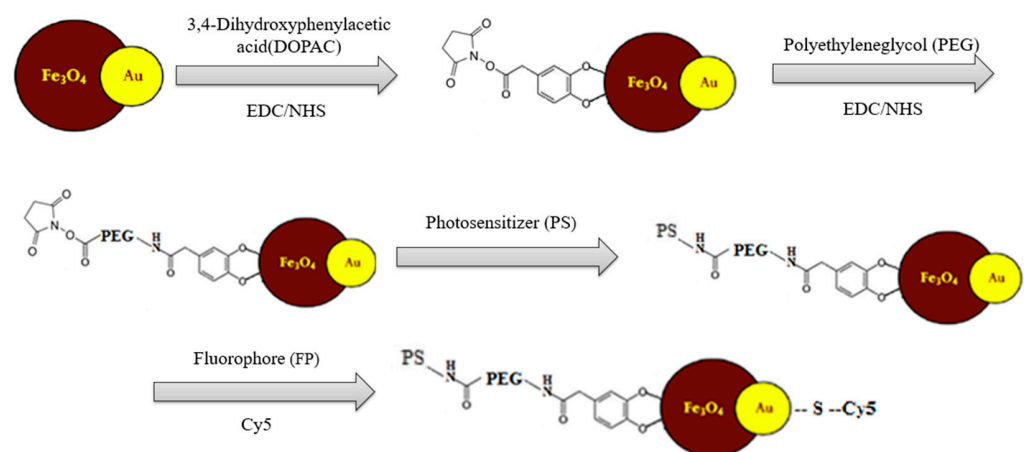


**Figure 1.** Systematic synthesis diagram of a bifunctional platform.

In the first stage, the synthesis of dimeric NPs  $\text{Fe}_3\text{O}_4$ -Au was carried out using joint thermal decomposition of  $\text{Fe}(\text{CO})_5$  and  $\text{HAuCl}_4$  (with in situ–formed Au particles) following the methodology taken from [11] with some modifications. Magnetite nanoparticles epitaxially grown on gold nanoparticles can be prepared by heating a mixture of 1-octadecene, oleic acid, oleylamine and 1,2-hexadecanediol to 120 °C in an inert gas atmosphere with stirring; introducing iron pentacarbonyl to the mixture; incubating the resulting mixture, followed by the introduction of a solution containing a mixture of gold chloride-hydrate and oleylamine in 1-octadecene’ preheating in an inert gas atmosphere, reheating to a temperature of 300–310 °C, keeping the heated mixture at 300–310 °C for 30–45 min; its subsequent cooling to room temperature, held in an inert gas atmosphere, keeping the mixture in the presence of air; adding monatomic alcohol to the mixture; and separating magnetite–gold nanoparticles using centrifugation.

A further synthesis step to obtain stable aqueous solutions of magnetite–gold nanoparticles involves stabilization carried out in several steps: The magnetite surface is covalently bonded to DOPAC (3,4-dihydroxyphenylacetic acid) with further activation using the carbodiimide (EDC/NHS) method, further stabilized by PEG (polyethylene glycol with COOH group) with further activation of the carboxyl group using the carbodiimide (EDC/NHS) method.

To functionalize the surface of  $\text{Fe}_3\text{O}_4$ -Au NPs, a FRET pair of chromophores was selected: a bacteriochlorine series photosensitizer (Figure 2, left) and a cyanine series fluorophore (Cy5) (Figure 2, right). The photosensitizer is immobilized via chemical conjugation to the stabilized magnetite surface. The derivative of the fluorescent dye Cy5 containing disulfide bonds is immobilized on the gold surface using the thiol group, namely by using the NHS ester of the fluorescent dye Cy5 with cystamine dihydrochloride with formation of disulfide bonds and further "cross-linking" to the gold surface.

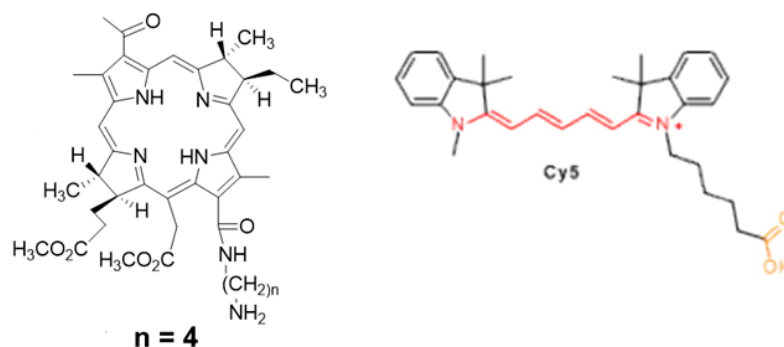


Figure 2. Photosensitizer  $n = 4$  (left); fluorophore Cy5 (right).

### 3. Results

As a result of the synthesis, dimeric dumbbell-shaped  $\text{Fe}_3\text{O}_4$ -Au NPs were obtained. A study of the crystal structure of dimeric  $\text{Fe}_3\text{O}_4$ -Au NPs using X-ray phase analysis yielded the following results. As can be seen from a diffraction picture (Figure 3), the relative intensity of all peaks, as well as their positions in the diffraction patterns, are in complete agreement with the structure of the  $\text{Fe}_3\text{O}_4$  magnetite (ICDD PDF-2 №00–019–0629). The same is true for the structure of Au gold (ICDD PDF-2 №03–065–8601) (yellow spheres). It should be noted that 100% correspondence of the spectrum "magnetic" component of all samples of low-frequency  $\text{Fe}_3\text{O}_4$ -Au to a type of cubic structure of spinel  $\text{Fd-3m}$  (magnetite type structure) is observed. Lattice parameters, crystallite sizes, and volume fractions were calculated for each phase from X-ray spectra (Table 1).

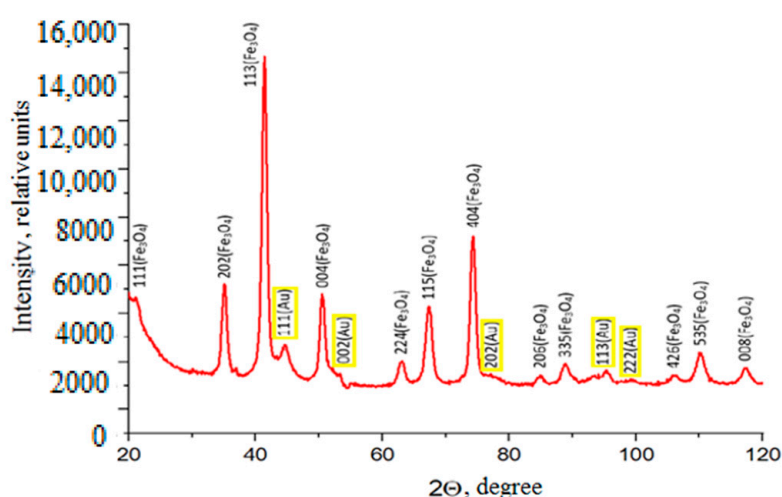
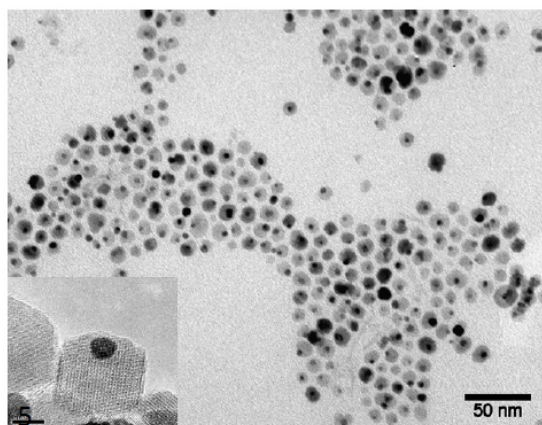


Figure 3. X-ray diffraction of  $\text{Fe}_3\text{O}_4$ -Au.

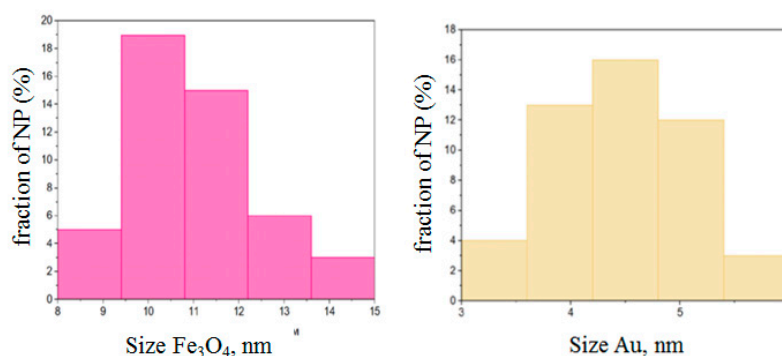
**Table 1.** Size, morphology, and structure of NPs Fe<sub>3</sub>O<sub>4</sub>-Au characterized using X-ray phase analysis and TEM.

TEM			X-ray Phase Analysis					
d, nm		Particle Shape	Volume Fraction, %		Crystallite Size, nm		Crystal Lattice Period, nm	
Fe <sub>3</sub> O <sub>4</sub>	Au		Fe <sub>3</sub> O <sub>4</sub>	Au	Fe <sub>3</sub> O <sub>4</sub>	Au	Fe <sub>3</sub> O <sub>4</sub>	Au
11	4	Spherical	99.3 ± 2.0	0.7 ± 0.2	12 ± 2.0	5 ± 1.0	0.8387 ± 0.0004	0.4064 ± 0.0004

The microphotographs (TEM) (Figure 4) show gold nanoparticles (darker) and magnetite nanoparticles (lighter) in pairs. In addition, it can be seen that the sample obtained did not contain aggregates of nanoparticles or free nanoparticles of magnetite and gold. Based on the data presented, we can conclude that the synthesis and subsequent purification resulted in the production of dimeric dumbbell-like Fe<sub>3</sub>O<sub>4</sub>-Au NPs with “double” chemistry, which, in turn, indicates the possibility of further obtaining nanoparticles with heterobifunctional surface properties.

**Figure 4.** TEM micrograph of dimeric Fe<sub>3</sub>O<sub>4</sub>-Au NPs and high-resolution micrograph.

According to the results of calculations, the average diameter of magnetite and gold particles was  $11 \pm 1.5$  and  $4 \pm 1$  nm, respectively (Figure 5).

**Figure 5.** Fe<sub>3</sub>O<sub>4</sub> and Au diameter size distribution for dimeric Fe<sub>3</sub>O<sub>4</sub>-Au nanoparticles.

The investigation of the structure of Fe<sub>3</sub>O<sub>4</sub>-Au NPs through high-resolution TEM and X-ray analysis revealed that the particles have defect-free single crystalline structure.

The investigation of the magnetostatic properties of Fe<sub>3</sub>O<sub>4</sub>-Au particles was carried out through hysteresis loop measurements at 300 K (Figure 6). The obtained values of saturation magnetization and coercive force were  $62.3 \pm 2.0$  and  $14 \pm 2$  mT respectively.

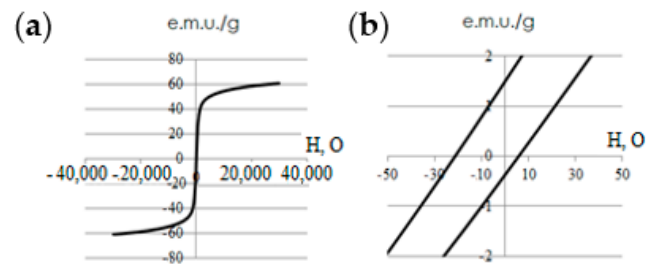


**Figure 6.** Magnetic properties of hybrid NP  $\text{Fe}_3\text{O}_4$ -Au: (a) hysteresis loops of ensembles at  $\text{MF} \pm 2$  Tesla at  $T = 300$  K and (b) their magnified near-zero regions.

The coercive force value based on the data in Figure 4 was less than 15 mT (14 mT); therefore, the synthesised  $\text{Fe}_3\text{O}_4$ -Au NPs can be considered as superparamagnetic. It is known that the saturation magnetization of nanosized magnetite [10] is 70–80 e.m.u./g, while that of magnetite is between 40 e.m.u./g. Thus, it can be assumed that the main phase in the studied sample is magnetite and not maghemite.

At each stage of the synthesis and modification of  $\text{Fe}_3\text{O}_4$ -Au NPs using dynamic light scattering, the particle size distribution was investigated, the values of which are given in Table 2.

**Table 2.** Hydrodynamic diameter.

Sample	$\text{Fe}_3\text{O}_4$ - Au/DOPAC	$\text{Fe}_3\text{O}_4$ - Au/DOPAC/PEG	$\text{Fe}_3\text{O}_4$ - Au/DOPAC/PEG/PS	$\text{Fe}_3\text{O}_4$ - Au/DOPAC/PEG/FP	$\text{Fe}_3\text{O}_4$ - Au/DOPAC/PEG/PS/FP
Size, nm	23.36	24.47	25.76	26.01	25.99
PDI	0.239	0.233	0.329	0.275	0.299

After the steps of conjugation with PS and FP, the absorption spectra of the  $\text{Fe}_3\text{O}_4$ -Au/DOPAC/PEG/PS and  $\text{Fe}_3\text{O}_4$ -Au/DOPAC/PEG/FP platforms and the spectra of pure solutions with PS and FP (DMSO solvent) were recorded. Using the  $\text{Fe}_3\text{O}_4$ -Au/DOPAC/PEG/PS system as an example, the absorption spectrum of this system with respect to the spectrum of pure PS/DMSO (Figure 7) is presented.

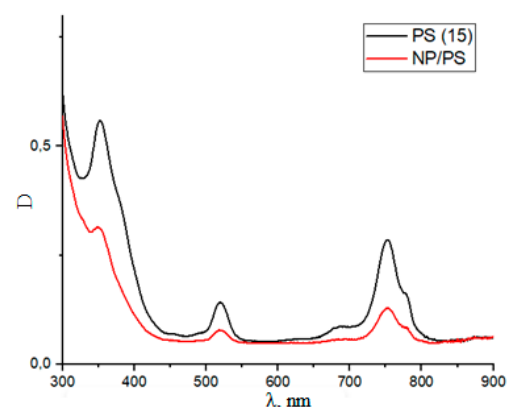


**Figure 7.** Absorption spectrum of the  $\text{Fe}_3\text{O}_4$ -Au/DOPAC/PEG/PS system with respect to the spectrum of pure PS/DMSO.

The values of the maxima of the pure PS absorption spectra correlate with the  $\text{Fe}_3\text{O}_4$ -Au/DOPAC/PEG/PS values (360 nm, 530 nm, and 750 nm). From this, we can conclude about the effective covalent conjugation of PS to the magnetic surface of NPs.

In vitro studies were performed on CT26 colon cancer cells (Figure 8) with an exposure time of up to 120 min, which showed that the  $\text{Fe}_3\text{O}_4$ -Au/PS and  $\text{Fe}_3\text{O}_4$ -Au/FP systems

exhibit a localized emission of fluorescence in their respective wavelength range in the time interval up to 120 min.

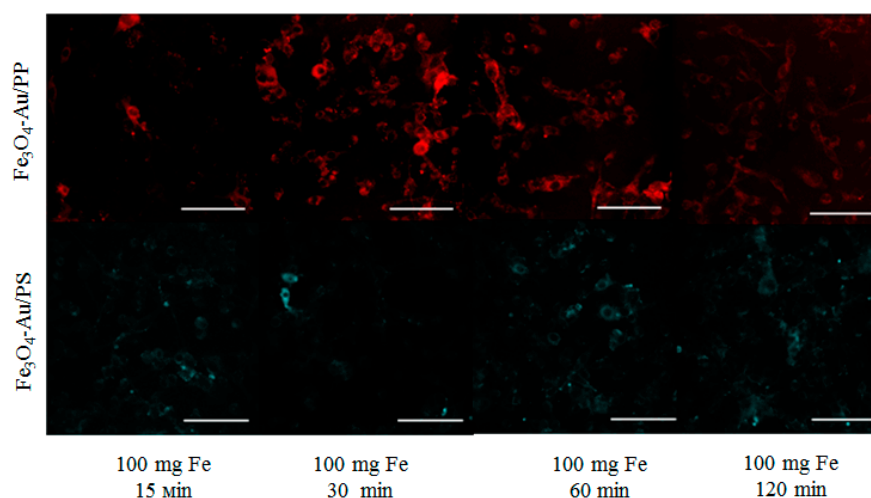


**Figure 8.** In vitro studies (CT26).

#### 4. Discussion

Depending on the temperature and size, ferromagnetic and ferrimagnetic particles can be in a multi-domain or single-domain ferromagnetic state and at  $d = 10\text{--}20$  nm in a superparamagnetic state. The latter, the most important for magnetic hyperthermia, is characterized by the magnetic ordering of atomic magnetic moments inside each magnetic nanoparticle. In this study, we synthesized a platform based on hybrid magnetite–gold nanoparticles with a size of about 15 nm. Such hybrid NPs have many advantages due to biocompatibility, magnetic properties, and the presence of two surfaces that can be modified. Previously, it was shown that such NPs prove themselves as contrast agents for MRI [11]. The presence of two surfaces, which increases the variability of various modifications, makes these NPs ideal candidates for use as targeted drug delivery platforms and also capable of providing a synergistic effect of magnetic hyperthermia and photothermal/photodynamic therapy due to the potential combination of their magnetic and plasmonic properties, provided that the size ratios of the  $\text{Fe}_3\text{O}_4$  and Au components are matched to the hybrid structure.

The study of the magnetic properties of the synthesized  $\text{Fe}_3\text{O}_4\text{-Au}$  NPs at room temperature showed that NPs can be considered superparamagnetic. According to the magnetization curves (Figure 6), in a field of 7 mT, the magnetization of NPs is  $7 \text{ Am}^2 \text{ kg}^{-1}$ . Given that NPs form conglomerates in an aqueous solution or culture medium, the total magnetization per conglomerate is higher. Thus, NP-FPs respond to various types of low-frequency (rotating/alternating) and constant magnetic fields in a magneto-optical system.

The main problem in the development of (bis)chromophore systems is the occurrence of a process of resonant energy transfer between the components of the conjugates, depending on the direction in which either the photodynamic or fluorescent properties of the systems deteriorate. Therefore, today the task is to find ways to minimize energy transfer.

The essence of the FRET (fluorescence resonance energy transfer) effect is that when two objects (donor and acceptor) approach each other and the fluorescence spectrum of the first one overlaps with the absorption spectrum of the second, energy is transferred nonradiatively, without the emission of photons [12].

Energy transfer is possible, not for any, but for strictly defined pairs of donors and acceptors. The main requirement for a donor–acceptor pair is the overlapping of the spectra. The donor must emit light of those wavelengths that the acceptor can absorb.

Another important criterion is the distance between the donor and acceptor. The efficiency of energy transfer is inversely proportional to the sixth power of the distance between them. The optimal distance between the donor and the acceptor can be determined by calculating the value of the Foerster radius, which is the maximum distance between the donor and acceptor molecules at which the FRET energy transfer occurs at a level of 50%.

To implement PDT, the photosensitizer and fluorophore must be selected in such a way that the pair is exchanged minimally via the donor–acceptor mechanism; otherwise, the fluorescent characteristics of the system deteriorate. Therefore, it is necessary to choose a PS and FP pair for which the critical Foerster radius is minimal. For this, it is necessary to calculate the quantum yield of generation of singlet oxygen by the photosensitizer, the quantum yield of fluorescence by the fluorophore, and the efficiency of energy transfer.

In order to select a PS and FP FRET pair, the following parameters must be taken into account: the quantum yield of PS singlet oxygen generation, the FF fluorescence quantum yield, and the energy transfer efficiency.

At this stage of the research, the minimum radius of Foerster was calculated with the following formula [12]:

$$R_0^6 = \frac{9000 \ln 10 k^2 \varphi_{D,0}^{fl}}{128 \pi^2 N_A n^4} \int_0^{\infty} F_D(\lambda) \varepsilon_A(\lambda) \lambda^4 d\lambda \quad (1)$$

The calculated minimum Foerster radius was 14.64 Å. The size of the synthesized particles was 15 nm, which is a satisfactory parameter to level out the possibility of energy transfer from PS to FP.

For further research, it is planned to carry out experiments and calculate the following:

- Fluorescence quantum yields of PS and PP using the formula

$$\varphi^{fl} = \varphi_R^{fl} \cdot \frac{S \cdot (1 - 10^{-AR}) \cdot n^2}{S_R \cdot (1 - 10^{-A}) \cdot n_R^2} \quad (2)$$

- Using the chemical trap method, the singlet oxygen generation for the selected PS;
- FRET energy transfer efficiency using the formula

$$k_{FRET} = \frac{1}{\tau} \cdot \left( \frac{R_0}{r} \right)^6 \quad (3)$$

Further investigation and characterization of the Fe<sub>3</sub>O<sub>4</sub>-Au/DOPAC/PEG/PS/FP system and the Fe<sub>3</sub>O<sub>4</sub>-Au/DOPAC/PEG/PS and Fe<sub>3</sub>O<sub>4</sub>-Au/DOPAC/PEG/FP conjugates in vivo are also planned.

## 5. Conclusions

1. The method of joint thermal decomposition of iron pentacarbonyl and gold tetrachloraurate allows one to obtain hybrid NP magnetite–gold of size  $11 \pm 1.5$  nm Fe<sub>3</sub>O<sub>4</sub> and  $4 \pm 1$  nm, stabilized by oleic acid;
2. A FRET pair of PP/PS (PS,  $n = 4/\text{Cy5}$ ) is selected, and the optical properties are studied;
3. The modification of the NPs with DOPAC and PEG, followed by EDC/NHS activation, allows for an efficient bonding of the PS to the magnetic surface of the NCs in a two-phase system (water-DMSO);
4. The immobilization of the FP disulfide derivative on the gold surface of the NPs is achieved using the thiol group;
5. The efficiency of the Fe<sub>3</sub>O<sub>4</sub>-Au/PS and Fe<sub>3</sub>O<sub>4</sub>-Au/FP systems is demonstrated through in vitro studies.

**Author Contributions:** Conceptualization, I.C. and M.A.; methodology, M.A.; software, M.A.; validation, M.A. and N.K.; formal analysis, I.C.; investigation, I.C. and M.S.; resources, M.A.; data curation, I.C. and M.S.; writing—original draft preparation I.C. and M.S.; writing—review and editing, N.K.; visualization, M.S.; supervision, N.K.; project administration, M.A.; funding acquisition, M.A. All authors have read and agreed to the published version of the manuscript.

**Funding:** This work was supported in part by the State Registration Theme AAAA-A21-121011290089-4 and 121041500039-8. The equipment was purchased within the framework of the Development Program of the Lomonosov Moscow State University.

**Institutional Review Board Statement:** This research received no external funding.

**Informed Consent Statement:** Not applicable.

**Data Availability Statement:** Not applicable.

**Conflicts of Interest:** The authors declare no conflict of interest.

## References

1. Yu, H.; Chen, M.; Rice, P.M.; Wang, S.X. Dumbbell-like bifunctional Au-Fe<sub>3</sub>O<sub>4</sub> nanoparticles. *Nano Lett.* **2005**, *5*, 379–382. [[CrossRef](#)] [[PubMed](#)]
2. Teranishi, T.; Inoue, Y.; Nakaya, M.; Oumi, Y.; Sano, T. Nanoacorns: Anisotropically Phase-Segregated CoPd Sulfide Nanoparticles. *J. Am. Chem. Soc.* **2004**, *126*, 9914–9915. [[CrossRef](#)] [[PubMed](#)]
3. Shi, W.L.; Zeng, H.; Sahoo, Y.; Ohulchanskyy, T.Y.; Ding, Y. A general approach to binary and ternary hybrid nanocrystals. *Nano Lett.* **2006**, *6*, 875–881. [[CrossRef](#)] [[PubMed](#)]
4. Glasser, N.; Adams, D.J.; Krausch, G. Janus particles at liquid-liquid interfaces. *Langmuir* **2006**, *22*, 5227–5229. [[CrossRef](#)] [[PubMed](#)]
5. Gu, H.W.; Yang, Z.M.; Gao, J.H.; Chang, C.K.; Xu, B. Heterodimers of nanoparticles: Formation at a liquid-liquid interface and particle-specific surface modification by functional molecules. *J. Am. Chem. Soc.* **2005**, *127*, 34–35. [[CrossRef](#)] [[PubMed](#)]
6. Choi, J.S.; Jun, Y.W.; Yeon, S.I.; Kim, H.C. Biocompatible Heterostructured Nanoparticles for Multimodal Biological Detection. *J. Am. Chem. Soc.* **2006**, *128*, 15983. [[CrossRef](#)] [[PubMed](#)]
7. Sokolov, K.; Follen, M.; Aaron, J.; Pavlova, I.; Malpica, A. Real-time vital optical imaging of precancer using anti-epidermal growth factor receptor antibodies conjugated to gold nanoparticles. *Cancer Res.* **2003**, *63*, 1999–2004. [[PubMed](#)]
8. Schultz, D.A. Plasmon resonant particles for biological detection. *Curr. Opin. Biotechnol.* **2003**, *14*, 13–22. [[CrossRef](#)] [[PubMed](#)]
9. El-Sayed, I.H.; Huang, X.; El-Sayed, M.A. Surface plasmon resonance scattering and absorption of anti-EGFR antibody conjugated gold nanoparticles in cancer diagnostics: Applications in oral cancer. *Nano Lett.* **2005**, *5*, 829–834. [[CrossRef](#)] [[PubMed](#)]
10. Gupta, A.K.; Naregalkar, R.R.; Vaidya, V.D.; Gupta, M. Recent advances on surface engineering of magnetic iron oxide nanoparticles and their biomedical applications. *Nanomedicine* **2007**, *2*, 23–39. [[CrossRef](#)] [[PubMed](#)]
11. Efremova, M.V.; Naumenko, V.A.; Spasova, M.; Garanina, A.S.; Abakumov, M.A.; Blokhina, A.D.; Melnikov, P.A.; Prelovskaya, A.O.; Heidelmann, M.; Li, Z.-A.; et al. Magnetite-Gold nanohybrids as ideal all-in-one platforms for theranostics. *Sci. Rep.* **2018**, *8*, 11295. [[CrossRef](#)] [[PubMed](#)]
12. Ushakova, E.V. Energy transfer of photoexcitation in the systems of quantum dots. *Sci. Tech. Bull. Inf. Technol. Mech. Opt.* **2008**, *51*, 283–288.

**Disclaimer/Publisher’s Note:** The statements, opinions and data contained in all publications are solely those of the individual author(s) and contributor(s) and not of MDPI and/or the editor(s). MDPI and/or the editor(s) disclaim responsibility for any injury to people or property resulting from any ideas, methods, instructions or products referred to in the content.